Heavy Metal Adsorption to a Chelating Resin in a Binary Solid Fluidized Bed

By *Jianzhong Yang* and *Albert Renken**

The addition of inert particles of lighter density and smaller diameter increases considerably the mass transfer coefficient in comparison to that of mono-component active particles at the same liquid velocity. This effect was applied to elimination of copper ions by adsorption on a chelating resin. An intensification of the film mass transfer coefficient in binary system leads to a 15 % increase of the usable adsorbent efficiency.

1 Introduction

Wastewater generated by electroplating contains a substantial amount of metal ions and the recovery of these metal ions is becoming of increasing importance for the protection of the environment. The development of efficient separation processes is leading to an increased interest in the engineering aspects. Many techniques can be used for pre-concentration of trace amounts of metal ions, and among these, adsorption of metal ions with chelating resins is an effective and powerful separation technology. Adsorption processes are traditionally carried out in fixed beds [1–5] due to the high concentration of solids and the obtainable uniform residence time. However since the wastewater to be treated often contains solid impurities leading to a plugging of the fixed bed, the liquid must be clear to avoid column blocking.

Another problem concerns shrinking and swelling of the resin during the adsorption/desorption processes resulting in poor liquid distribution caused by channeling and formation of dead zones [6–7]. Therefore many experimental studies have been conducted in fluidized beds, which allow treatment of turbid liquids while avoiding the channeling problems [8–14].

For a proper design of the fluidized bed adsorber, an adequate mathematical model is required which takes into account the hydrodynamics and adsorption kinetics. Menoud et al [15] studied the adsorption kinetics of a chelating resin (Chelamine JPS-Chimie, Neuchâtel, Switzerland [16]) and found that the overall adsorption rate is limited by external mass transfer. Therefore intensification of the mass transfer should increase the performance of the fluidized bed adsorber for such an adsorption system.

According to our previous work [17], the addition of inert particles of heavier density and smaller diameter could be used to increase the film mass transfer coefficient. In this work, this technique is applied to the aforementioned system. A comparison is made of copper ion removal in mono-component and binary solid systems, thereby providing the information to understand the changing tendency of adsorption process at different mass transfer coefficients and to evaluate the influence extent of small/heavier inert particles on adsorption performance.

[*]   Dr. J. Yang, Prof. Dr. A. Renken, Laboratory of Chemical Reaction Engineering, Swiss Federal Institute of Technology, CH-1015 Lausanne, Switzerland.

2 Adsorption Model in a Fluidized Bed

The governing equations for the adsorption of copper ion in a fluidized bed can be derived on the base of the research results of the equilibrium isotherm and hydrodynamics of liquid and solid particles [15]. In the development of the mathematical model, several simplifying assumptions are made as follows :

- Adsorption rate is limited by a liquid film resistance and surface reaction.
- Surface reaction between adsorbate and adsorption site is described by a reversible second order reaction. Adsorption equilibrium behavior is represented by the Langmuir isotherm.
- Adsorbent particles are spherical with a mean diameter d_p. These particles are relatively immobile and distributed uniformly in the column.
- Axial dispersion of liquid is negligible.

A material balance of the cation in the mobile phase for such a system gives rise to[1]

$$\varepsilon_r \frac{\partial c}{\partial t} = -u \frac{\partial c}{\partial z} - R_i \tag{1}$$

The adsorption rate from the bulk solution to the surface of particles is :

$$R_i = k_L a (c - c_i) \tag{2}$$

Where a is the surface area of the particles per reactor unit volume; c is the bulk concentration; k_L, the film mass transfer coefficient; the temporal point concentration of solute c_i can be calculated by a mass balance at the liquid-solid interface:

$$\varepsilon_r \frac{\partial c_i}{\partial t} = k_L a (c - c_i) - (1 - \varepsilon_r) \rho_p \frac{\partial q}{\partial t} \tag{3}$$

The reaction rate in the solid phase is related to the interface concentration c_i and described by the Langmuir isotherm:

$$\frac{\partial q}{\partial t} = k_f (c_i (q_m - q) - K_d q) \tag{4}$$

$$K_d = \frac{k_r}{k_f} \tag{5}$$

Where the parameters k_f and k_r are the rate constants of forward and reverse reaction, respectively; K_d, the dissociation constant; q_m, maximum capacity of resin.

The initial and boundary conditions would be

$$c = 0 \quad q = 0 \quad at \ t = 0 \tag{6}$$

$$c = c_0 \quad at \ z = 0, \ t > 0 \tag{7}$$

$$\frac{\partial c}{\partial z} = 0 \quad at \ z = h, \ t > 0 \tag{8}$$

The mass balance for the adsorbate is a partial differential equation. This equation can be reduced to an ordinary differential equation using the finite difference method. It is assumed that a fluidized bed of total volume V can be divided into N equal size cells in series and that the liquid flowing upwards passes through the bed. Furthermore, in order to compare the model with different experimental results, it is convenient to use the following dimensionless variables:

$$f = \frac{c}{c_0} \tag{9}$$

$$\xi = \frac{q}{q_0} \tag{10}$$

$$\theta = \frac{t}{\tau_m} = \frac{Q c_0 t}{m q_0} \tag{11}$$

$$\tau_m = \frac{mq_0}{Qc_0} \tag{12}$$

The variables f and ξ are dimensionless concentrations in liquid and solid phases respectively; θ, the dimensionless time; τ_m, the time required for saturating all the resin in the reactor; c_0, the concentration of cation at the inlet of the column; q_0, the dynamic capacity of the resin which is in equilibrium with c_0; m, the mass of dry resin; Q, the flow rate of liquid.

After transformation with these dimensionless variables, the mass balance for the jth cell becomes:

$$\frac{df_j}{d\theta} = N \cdot \psi \cdot (f_{j-1} - f_j) - DaI_{kL} \cdot \psi \cdot (f_j - f_{i,j}) \tag{13}$$

$$\frac{df_{i,j}}{d\theta} = DaI_{kL} \cdot \psi (f_j - f_{i,j}) - \psi \frac{d\xi_j}{d\theta} \tag{14}$$

$$\frac{d\xi_j}{d\theta} = \frac{DaI_{kf}}{\xi_m} (f_{i,j}(\xi_m - \xi_j) - (\xi_m - 1)\xi_j) \tag{15}$$

While developing the differential equations, several dimensionless groups are introduced. Some explications for these parameters are given as follows:

● DaI_{kL} is a Damköhler number, which is defined by:

$$DaI_{kL} = \frac{k_L a \tau}{\varepsilon_r} \tag{16}$$

DaI_{kL} represents the number of film mass transfer units which is the ratio between the hydraulic residence time and a characteristic time of adsorption [18]. For a fixed residence time, if the value DaI_{kL} is larger, the adsorption will be carried

out at a higher rate and the concentration of solute at the exit of the column is lower.

● DaI_{kf} is another Damköhler I number, which is given by:

$$DaI_{kf} = \frac{k_f q_m m}{Q} \tag{17}$$

This is an expression for the number of transfer units due to the intrinsic adsorption kinetics.

Two transfer units DaI_{kL} and DaI_{kf} can be combined as the resistances in series to yield the overall number of transfer units [19]:

$$\frac{1}{DaI} \approx \frac{1}{DaI_{kL}} + \frac{1}{DaI_{kf}} \tag{18}$$

● ψ is a residence time number required to saturate all the resin in the reactor:

$$\psi = \frac{\tau_m}{\tau} = \frac{mq_0}{\varepsilon_r c_0 V} \tag{19}$$

● ξ_m is an equilibrium factor which is defined by:

$$\xi_m = \frac{q_m}{q_0} = \frac{K_d}{c_0} + 1 \tag{20}$$

The equilibrium factor depends on the concentration of solution c_0 at the inlet of the column for a continuous adsorption process. If $\xi_m \to \infty$, the concentration of solution c_0 is in the linear region of the Langmuir isotherm curve; if $\xi_m \to 1$ the dynamic capacity q_0 approximates to the maximum capacity of the resin, the c_0 and q_0 are in the plateau region of the Langmuir isotherm curve.

The response at the exit of the column is given by the concentration f_N and Eqs. (13), (14) and (15) must be solved simultaneously subject to the boundary conditions ($f_{j-1} = 1$ when $j = 1$ and $\theta > 0$) and the initial conditions (f_j, $f_{i,j}$, and q_j are zero when $\theta = 0$ ($1 \le j \le N$)).

This two-resistance model can be used as a sole resistance-limiting model by giving a high value for another resistance coefficient. When the reaction rate is instantaneous, only the film mass transfer resistance controls the adsorption rate, the temporal point concentration c_i in Eq. (2) can be directly calculated with the Langmuir equilibrium:

$$c_i = \frac{qK_d}{q_m + q} \tag{21}$$

Using this theoretical framework and a SimuSolv program (Dow Chemical Company) [20], the contributions of mass transfer processes and kinetics may be estimated and compared with the experimental results.

3 Experimental

3.1 Materials

The adsorbent used in this study is a resin, Chelamine Standard® (JPS-Chimie, Neuchâtel, Switzerland) [16]. The

adsorbate is a copper ion solution prepared with penta-hydrate cupric sulfate (Fluka-AG, Buchs, Switzerland). The inert particles are glass beads (Microbeads, Brugg, Switzerland). The mean particle sizes and other properties for glass beads and resins are summarized in Tab. 1.

3.2 Experimental Protocol and Methods

The fluidized bed reactor previously used [15] is modified and used for monitoring the effect of inert particles on the adsorption process. A column is comprised of five Plexiglas elements (52 mm inner diameter and 102 mm height) which are designed with a thermostatic double jacket. During the adsorption experiment, the copper ion solution (~30 ppm) in the tank is circulated through a heat exchanger using a peristaltic pump, then fed into the column. The flow rate is measured with a calibrated rotameter. The *pH* is measured with an on-line *pH* meter and the temperature is measured with a thermocouple, the results are recorded automatically with a data acquisition system (LabVIEW for windows, version 3.0, National Instruments Corporation).

To determinate the concentration of the copper ion, the effluent at the outlet of the column is continuously withdrawn by a peristaltic pump. In parallel, an EDTA solution (0.1 M) is supplied at the same flow rate, thus complex solution of copper ion-EDTA produces a measurable color. The optical density of the complex solution of copper ion-EDTA is measured with an on-line UV/VIS spectrophotometer (Diode array spectrophotometer 8452A, Hewlett Packard) at 732 nm [20]. The results are recorded by a computer and converted to concentration according to the Lambert-Beer law [21].

The color of the resin changes from yellow to green and then becomes dark blue during the adsorption process. The resin at the bottom of the column is loaded initially and this can be observed clearly from the color change. The resin particles shrink due to the loading of copper ion, therefore the height of the suspension layer decreases during the adsorption process. The mean height is taken into account for calculating the reactor volume. The diameter of loaded resin (340 μm) is used to determinate the mass transfer surface area.

For comparison, the operating conditions are kept identical for the two kinds of experiments. The only difference is that the glass beads (30 ml) are added to the column for the experiments with the binary system. The detailed operating conditions for experiments MIX3 and NOR5 are given in Tab. 2.

Table1. Properties of solid particles in binary system.

Parameter	Symbol	Value	Units
Resin (Chelamine)			
Mean volumetric diameter	d_p	414	μm
Particle porosity	ε_p	0.81	–
Mass of dry resin per unit volume of swollen resin	ρ_{ps}	158.4	kg·m^{-3}
Apparent density	ρ_{ap}	1064	kg·m^{-3}
Archimedes number	Ar	46	–
Inert particles (glass beads)			
Mean volumetric diameter	d_p	103	μm
Apparent density	ρ_p	2450	kg·m^{-3}
Archimedes number	Ar	15	–

4 Results and Discussion

Typical adsorption experimental results (points) are shown as a function of dimensionless time θ in Fig.1 and Fig.2. The *pH* profiles (dotted curves) are also given in the same figures.

A comparison is made firstly between the film mass transfer and intrinsic adsorption kinetics with the two-resistance model. By using the film mass transfer coefficient and the intrinsic forward rate constant which are obtained with simulation, the number of transfer units for film mass transfer DaI_{kL} and the number of transfer units for the intrinsic adsorption kinetics DaI_{kf} are calculated by Eq. (16) and Eq.

Table 2. Operation conditions.

| Operating parameters	Symbol	MIX3	NOR5	Units
Operation temperature	T	20.0	20.0	°C
pH for preconditioning of resin	pH_0	13	13	–
Height of free settled bed	h_0	0.118	0.108	m
Height of resin in fluidized bed	h	0.20	0.20	m
Voidage of reactor	ε_r	0.662	0.662	–
Liquid flow rate	Q	3.963·10^{-6}	3.900·10^{-6}	m^3·s^{-1}
Volume of reactor	V	4.248·10^{-4}	4.248·10^{-4}	m^3
Residence time	τ	71	72	s
Feed concentration of Cu^{2+}	c_0	0.4637	0.4809	mol·m^{-3}
Mass of dry resin	m	0.0227	0.0227	kg
Volume of free settled resin	V_0	2.0·10^{-4}	2.0·10^{-4}	m^3
Voidage of free settled resin	ε	0.334	0.334	–
Volume of free settled glass beads	V_{0g}	3.0·10^{-5}	–	m^3
Surface area per unit volume	a	3303	3303	m^2·m^{-3}
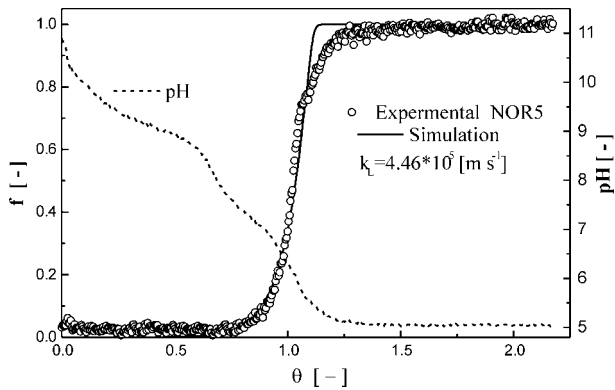
Figure 1. Experimental data and modeling of normal adsorption of copper ion onto Chelamine resin.
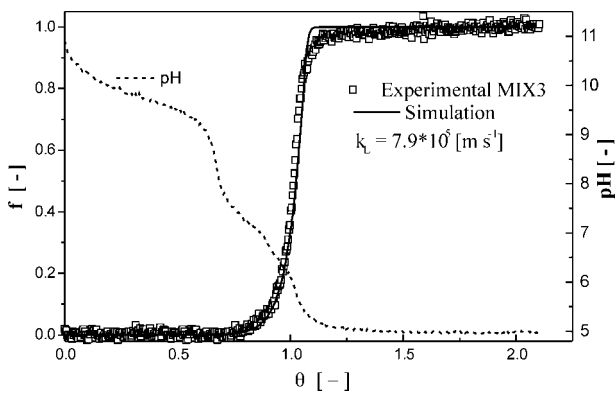

Figure 2. Experimental and modeling results on the adsorption of Cu^{2+} onto Chelamine resin in the suspension of glass beads.

(17), respectively. The number of transfer units for the adsorption of copper ion on chelating resin (experiment NOR5) is found to be respectively 145 for DaI_{kf}, and 16 for DaI_{kL}. The overall number of transfer units DaI is calculated by Eq. (18), and has a value of 14. The number of transfer units for the intrinsic adsorption kinetics is about 9 fold higher than that for the film mass transfer. This indicates that the surface interaction is much faster than the film mass transfer and the overall adsorption rate is limited mainly by the film mass transfer for this system.

Since the film mass transfer resistance appears to be the controlling step for the overall adsorption rate, a one parameter model, in which only the film mass transfer is considered, is sufficient. The simulated curve describes the experimental data reasonably well, however, at the second breakthrough point, the two-resistance model fits better than the one resistance model (results not shown here) [20]. This suggests that the surface reaction becomes more important when the resin approaches saturation. In other words, there is a lateral interaction between adsorbed molecules, the assumption in the Langmuir model does not held true for this case. Since the volume of resin particles decreases with loading of copper ion, the adsorbed cations exert an effect on the interaction between new solute and active sites. A

decrease of k_f is possibly due to steric change of the resin or pore blockage by adsorbed cations. Koloini and Zumer [22] thought that after approximately 80 % of the resin capacity is exhausted the internal resistance to the adsorption process becomes important and the overall rate of the ion exchange decreases continuously. This behavior has been observed by other authors [18, 23] for protein adsorption in fixed beds. Therefore the two-resistance model is recommended for the following process simulation.

For the sake of comparison of the influence of inert particles on the film mass transfer coefficient, the forward rate constant and isotherm equilibrium constant are assumed to be fixed (k_f =$2 \cdot 0^{-2}$ m^3·mol^{-1}·s^{-1}, K_d = 0.0067 mol m^{-3}) [14]. The liquid film mass transfer coefficient is a free parameter, with a value determined by fitting the experimental data. As typical examples simulation results for a mono-component (NOR5) and a binary-mixture systems (MIX3) are shown in Fig.1 and Fig.2 respectively. The prediction of the model (curve) for fluidized bed performance results in a good agreement. The values for the mass transfer coefficient obtained with the simulations are $4.4 \cdot 10^{-5}$ (m·s^{-1}) for the mono-component system and $7.9 \cdot 10^{-5}$ (m·s^{-1}) for the binary mixture system. The film mass transfer coefficient is substantially higher in the binary-mixture system and this confirmed once again that the small/heavier inert particles can be applied to intensify the external mass transfer.

From the engineering point of view, the main requirement for rational design is an estimate of the dynamic capacity of the fluidized bed. Assuming that the adsorption column is used to remove a trace impurity from a stream, a maximum permissible concentration at the outlet of the column is required, due to the legislation for the provision of water contamination. For example, the permissible concentration of Cu^{2+} in the effluent water should be less than 0.5 ppm in Switzerland and Germany [24–25]. During the adsorption process, the effluent concentration at the outlet of the column increases gradually. The operation should be stopped when the effluent concentration reaches the maximum permissible concentration. The corresponding time may be called break time θ_b. The dynamic capacity of the bed depends on the break time and can be calculated from the following mass balance:

$$q = q_0 \int_0^{\theta_b} (1-f)d\theta - \frac{\varepsilon_r c_0}{m} \int_0^f V df \qquad (22)$$

Assuming that the quantity of metal ions in the liquid phase of the reactor is negligible compared to the adsorbed one, the usable fraction of the total capacity of adsorbents may be expressed using the following approximate relationship:

$$\eta = \frac{q}{q_0} \approx \int_0^{\theta_b} (1-f)d\theta \qquad (23)$$

Defined in this way, the usable fraction of the total capacity of adsorbents in the column can be represented by the shaded area in Fig 3.
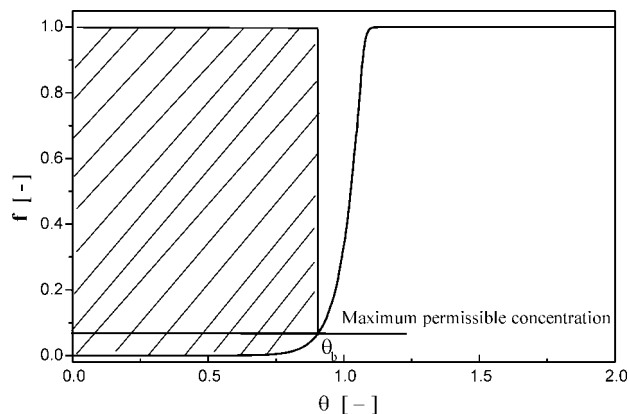
Figure 3. Usable efficiency of total capacity of adsorbents in the column.

Figure 5. Influence of mass transfer coefficient on usable efficiency of adsorbents in the column.

For given operating conditions, the effluent concentration at the outlet of column changes during the adsorption process and forms an asymptotic breakthrough. The shape of the breakthrough curve is depending on the mass transfer rate as shown in Fig. 4. With increasing mass transfer coefficient, the effluent concentration at the outlet of the column decreases and the break time θ_b is postponed. Therefore the usable fraction of absorbents increases with increasing the mass transfer coefficient. Due to the higher mass transfer rate in a binary fluidized system, the break time increases from θ_{b1} to θ_{b2}, resulting in a 15% higher usable fraction of the adsorbent.
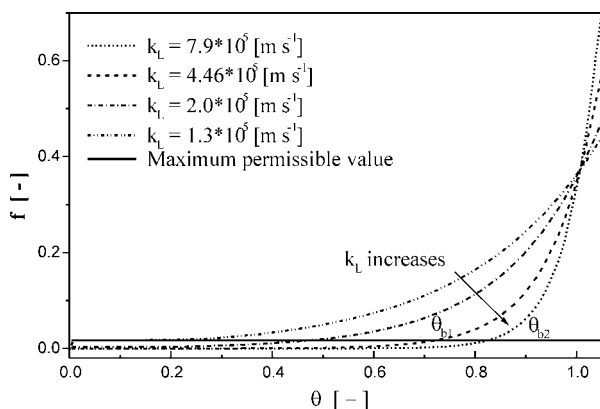

Figure 4. Influence of mass transfer coefficient on break time.

The influence of the mass transfer coefficient on the break time and therefore the usable fraction of the adsorbent is summarized in Fig. 5, where the relationship between the usable fraction η is plotted as function of the mass transfer coefficient k_L in the fluidized bed adsorber. As shown in Fig. 5 for the given operating conditions of experiment Mix3, the usable fraction is nearly zero, if the mass transfer coefficient is less then $1.3 * 10^{-5}$ (m/s). That means that the concentration at the outlet of the column is higher than the permissible concentration at the beginning of the operation process. With increasing mass transfer coefficient, the usable fraction η increases sharply in the range of $k_L = 1.3 \sim 3 * 10^{-5}$ (m/s), and is then followed by a gradual increase at higher values.
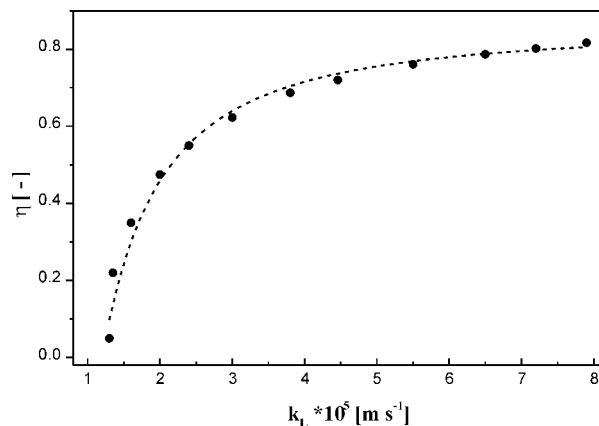
5 Conclusions

Adsorption processes of copper ions onto a chelating resin in fluidized beds are studied experimentally and simulated with theoretical models. Comparison of the number of transfer units for film mass transfer and the number of transfer units for intrinsic adsorption kinetics indicate that the overall adsorption rate is limited mainly by the film mass transfer resistance for this system.

Small/heavier inert particles (glass beads) are used to mix with the resin particles during the adsorption of metal ion in the liquid fluidized bed. The experimental and theoretical results prove that the addition of inert glass beads exerts a significant positive effect on the film mass transfer coefficient.

For an adsorption process in which surface film resistance is the limiting step, an increase of the film mass transfer coefficient will result in a decrease of the effluent concentration at the outlet of the reactor and a postponement of the break time θ_b or prolongation of the operating time resulting in a significant increase of the usable fraction of adsorbent η as defined in Eq.(23).

Acknowledgement

Symbols used

a	[m^2 m^{-3}]	surface area per unit volume of reactor
Ar	[–]	Archimedes number,
		$= d_p^3 (\rho_{ap} - \rho)\rho g / \mu^2$
c	[mol m^{-3}]	bulk concentration of liquid in reactor
c_i	[mol m^{-3}]	cation concentration at the liquid–solid interface

c_0	[mol m^{-3}]	cation concentration at inlet of the reactor
d_p	[m]	mean particle diameter
DaI_{kf}	[–]	Damköhler I number $= \frac{k_f \cdot q_m \cdot m}{Q}$
DaI_{kL}	[–]	Damköhler I number $= \frac{k_L \cdot a^* \cdot \tau}{\varepsilon_r}$
f	[–]	dimensionless liquid phase concentration
h	[m]	height of particle layer in fluidized bed
h_0	[m]	height of particle layer in free settled bed
K_d	[mol m^{-3}]	Langmuir isotherm equilibrium constant
k_f	[m^3 mol^{-1} s^{-1}]	rate constant of forward reaction
k_L	[m·s^{-1}]	liquid-solid mass transfer coefficient
k_r	[s^{-1}]	rate constant of reverse reaction
m	[kg]	mass of dry resin
q	[mol· kg^{-1}]	concentration of adsorbate in adsorbent
q_m	[mol· kg^{-1}]	maximum adsorption capacity of resin
q_0	[mol· kg^{-1}]	dynamic capacity of resin which is in equilibrium with c_0
Q	[m^3 s^{-1}]	liquid flow rate
t	[s]	time
T	[°C]	temperature
u	[m·s^{-1}]	superficial liquid velocity
V_0	[m^3]	volume of free settled resin particles in the reactor
V_{0g}	[m^3]	volume of free settled glass beads in the reactor
V	[m^3]	volume of the reactor
z	[m]	axial coordinate along the column

Greek symbols

ε_0	[–]	settled bed porosity
ε_p	[–]	particle porosity
ε_r	[–]	reactor porosity
η	[–]	usable efficiency of total capacity of adsorbents
θ	[–]	dimensionless time
θ_b	[–]	break dimensionless time
ρ	[kg·m^{-3}]	density of liquid solution
ρ_{ap}	[kg·m^{-3}]	apparent particle density
ρ_{ps}	[kg·m^{-3}]	mass of dry resin per unit volume of swollen resin
μ	[mPa·s]	liquid viscosity
τ	[s]	hydraulic residence time
τ_m	[s]	time required for saturating all the resin in reactor
ξ	[–]	dimensionless solid phase concentration
ψ	[–]	resistance time number to saturate all the resin in reactor

References

[1] McDougall, G. J.; Fleming, C. A., Extraction of precious metals on activated carbon, in Ion Exchange and Sorption Processes in Hydrometallurgy, Ed. by Streat, M. and Naden, D., *Critical Reports on Applied Chemistry 19* (1987) pp. 56–126.

[2] Clifford, D.; Zhang, Z., Modifying ion exchange for combined removal of uranium and radium, J. Am. *Water Works Assoc. 86* (1994) pp. 214–227.

[3] Becker, N. S. C.; Eldridge, R. J., Selective recovery of mercury(II) from industrial wastewaters. II. Anion exchange of Hg(II) chlorocomplexes, *React. Polym. 22* (1994) pp. 131–138.

[4] Petruzzelli, D.; Tiravanti, G.; Santori, M.; Passino, R., Chromium removal and recovery from tannery wastes: Laboratory investigation and field experience on a 10 m^3/d demonstration plant, *Wat. Sci. Tech. 30* (1994) pp. 225–233.

[5] Petruzzelli, D.; Passino, R.; Tiravanti, G., Ion exchange process for chromium removal and recovery from tannery wastes, *Ind. Chem. Eng. 34* (1995) pp. 2612–2617.

[6] Yang, J.; Menoud, P., Adsorption de métaux lourds à l'aide de la résine Chelamine, Compte-rendu 1, EPF, Lausanne 1994.

[7] Schmidt, V., Développement d'un système fluidisé pour la récupération des métaux lourds des eaux industrielles par des résines chélatantes, Thèse No. 1247, IGC-DC, Ecole Polytechnique Fédérale, Lausanne 1994.

[8] Biscans, B., Chromatographie d'échange d'ions en couche fluidisée. Extraction des protéines du lactosérum, Thèse ENSIGC, Toulouse 1985.

[9] Biscans, B.; Riba, J. P.; Couderc, J. P., Continuous equipment for ion exchange in a fluidized bed. Prospects and problems, *Int. Chem. Eng. 28* (1988) pp. 248–256.

[10] Han, K. N; Liu, J., Removal of cadmium and zinc ions by liquid fluid-beds, in: *Emerging Proc.Technol. Cleaner Environ.* Proc. Symp., Soc.Min. Metall. Expl., Littleton. Colo 1992, pp. 175–183.

[11] Zarraa, M. A., Mass transfer during the removal of dissolved heavy metals from wastewater flows in fluidized beds of ion exchange resins, *Chem. Eng. Technol. 15* (1992) pp. 21–25.

[12] Nakamura, S.; Ito, Y.; Iwafuchi, K.; Shirakashi, M., Improvements in uranium adsorption ability of a circulating fluidized bed adsorber, *J. Japan Chem. Eng. 27* (1994) pp. 32–38.

[13] Huang, L.; Hao, O. J.; Chen, J. M.; Buglass. R. L., Metal toxicity on sulfate reducing bacteria, in: *Proceedings of 25th Mid-Atlantic Ind. Waste Conf.* (1995) pp. 541–550.

[14] Menoud, P., Récupération de métaux lourds par une résine chélatante, Thèse No. 1563, IGC-DC, Ecole Polytechnique Fédérale, Lausanne 1996.

[15] Menoud, P.; Cavin, L.; Renken, A., Modeling of heavy metals adsorption to a chelating resin in a fluidized bed reactor, *Chem. Eng. Proc. 37* (1998) pp. 89–101.

[16] Jeanneret-Gris, G., Brevet européen, 0362325 1990.

[17] Yang, J.; Renken, A., Intensification of mass transfer in liquid fluidized beds with inert particles, *Chem. Eng. Proc. 37* (1998) pp. 537–544.

[18] Boyer, P. M.; Hsu, J. T., Effect of ligand concentration on protein adsorption in dye-ligand adsorbents, *Chem. Eng. Sci. 47* (1992) pp. 241–251.

[19] Arnold, F. H.; Blanch, H. W., Analysis of affinity Chromatography. II. Rate theory and the measurement of biological binding kinetics, *J. Chromat. 355* (1986) pp. 13–27.

[20] Yang, J., Hydrodynamics and liquid-solid mass transfer in non-conventional fluidized beds, Thesis No. 1919, IGC-DC, Ecole Polytechnique Fédérale, Lausanne 1998.

[21] Cavin, L., Etude cinétique de la désorption de métaux lourds sur la résine Chélamine par complexation avec un polymère soluble, Travail de diplôme, EPF, Lausanne 1996.

[22] Koloini, T.; Zumer, M., Ion exchange with irreversible reaction in deep fluidized beds, *Canadian Chem. Eng. 57* (1979) pp. 183–190.

[23] Horstmann, B. J.; Chase, H. A., Modeling the affinity adsorption of immunoglobulin G to protein immobilized to agarose matrices, *Chem. Eng. Res. Des. 67* (1989) pp. 243–254.

[24] *Confédération Helvétique, Ordonnance sur le déversement des eaux usées, Ordonnance 814.225.21*, (1975) pp. 1–16.

[25] Hartinger, L., *Handbuch der Abwasser und Recycling Technik, 2nd ED.* Carl Hanser Verlag, München, Wien 1991.